(will be inserted by hand later)

Research Note

An optical inverse-Compton hotspot in 3C 196?

M.J. Hardcastle

Department of Physics, University of Bristol, Tyndall Avenue, Bristol BS8 1TL, UK (m.hardcastle@bristol.ac.uk)

Version of May 16, 2001

Abstract. Several hotspots of FRII radio sources have previously been detected in the X-ray at a flux level consistent with the X-rays being due to inverse-Compton scattering of radio synchrotron photons ('synchrotron self-Compton'), if the magnetic fields in the hotspots are close to their equipartition values. However, the number of hotspots compact and bright enough to exhibit detectable X-ray emission is small, so it is worth searching for synchrotron self-Compton emission in the optical, in spite of the obvious observational difficulties of such an approach. In this note I report on a possible detection of an optical inverse-Compton hotspot in a deep *Hubble Space Telescope* observation of the distant quasar 3C 196, at a level which implies a hotspot magnetic field strength close to equipartition if the electrons have a low-energy cutoff around $\gamma \sim 500$.

Key words. galaxies: active – radiation mechanisms: non-thermal – quasars: individual: 3C 196

1. Introduction

The relativistic electron population responsible for synchrotron emission in extragalactic radio sources necessarily scatters incoming photons up to higher energies by the inverse-Compton process. Possible source photon populations include the microwave background, starlight from the host galaxy, photons from the active nucleus and the synchrotron photons themselves; different populations will dominate in different regions of the source. In the compact hotspots of powerful double (FRII) radio sources, the dominant component is expected to be the synchrotron photons, and the so-called 'synchrotron self-Compton' (SSC) process should accordingly dominate the inverse-Compton emissivity.

Observations of SSC emission are important because they allow us to make a measurement of the magnetic field strength in the hotspot. We know the synchrotron flux density and the dimensions of the hotspot, which give us the synchrotron emissivity and photon energy density. A measurement of the inverse-Compton emissivity then tells us about the electron energy density, allowing us to infer the magnetic field strength from the observed synchrotron emission.

However, SSC emission from hotspots is expected to be faint. So far there are four convincing cases of inverse-Compton emission detected with X-ray observations, in the radio galaxies 3C 405 (Harris, Carilli & Perley 1994; Wilson, Young & Shopbell 2000), 3C 295 (Harris et al. 2000), 3C 123 (Hardcastle et al. 2000) and the quasar 3C 263 (Hardcastle et al. in preparation); these detections are consistent with a hotspot magnetic field strength close to the minimum energy or equipartition value. These objects represent some of the brightest well-studied hotspots in the sky, and the faintest of them approaches the detection limit of long *Chandra* observations. There may be fewer than ten objects in the entire sky that have hotspots whose SSC emission is detectable at a useful level in the X-ray with the present generation of instruments.

Because the spectrum of SSC emission is expected to be similar to that of synchrotron emission, SSC emission in the optical ought to be detectable at flux levels higher than those seen in the X-ray. However, there are several difficulties with observing this in practice. Firstly, in many cases, the high-frequency radio/sub-mm/IR spectrum of hotspots is poorly known, which means that it is hard to say whether an optically detected hotspot is synchrotron or inverse-Compton — a number of sources have well-known optical synchrotron hotspots. For example, it is not clear whether the optical hotspot of 3C 295 detected by Harris et al. (2000) is synchrotron or SSC in nature. Secondly, because the increase in frequency in the SSC process goes as γ^2, SSC at low frequencies probes low-energy electrons (with $\gamma \lesssim 1000$) and we typically do not know much about the radio emission from these electrons; our models are accordingly uncertain. And finally there are practical difficulties; emission from the hotspots is often too faint to be seen in the optical against the background from the host galaxy or active nucleus. However,

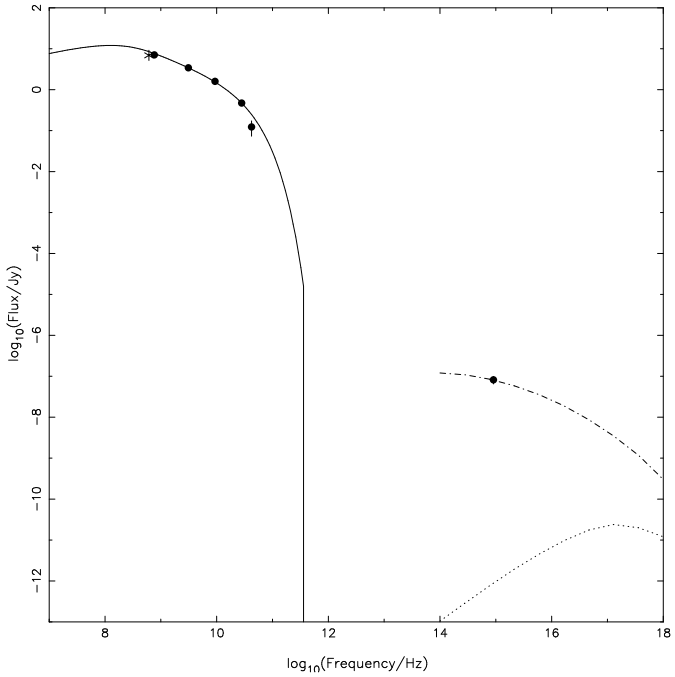

Fig. 2. The synchrotron and inverse-Compton spectrum of 3C 196's N hotspot. Radio data are from Table 1, and are plotted in the rest frame of the quasar. The optical data point is discussed in the text. The dot-dashed line shows a synchrotron self-Compton spectrum fitted to the data, using a model with equipartition magnetic field strength and $\gamma_{\rm min} = 420$. The dotted line is the contribution from inverse-Compton scattering of the microwave background for these parameters.

detection of optical SSC emission is still possible in principle, and could give us valuable information about the magnetic field strengths and low-energy electron populations in hotspots. In this note I report on a possible detection of optical SSC emission from the distant quasar 3C 196. Except where otherwise stated, I use a cosmology with $H_0 = 65$ km s^{-1} Mpc^{-1}, $\Omega_{\rm m} = 0.3$, $\Omega_\Lambda = 0.7$.

2. Observations

3C 196 is a $z = 0.871$ quasar with a compact, FRII-like radio structure (Laing 1982; Lonsdale & Morison 1983, hereafter LM; Brown 1990). It came to our attention as a possible target for *Chandra* observations because of its very bright, compact hotspots, with flux densities around 2 Jy at 5 GHz (LM). However, investigation of the available high-frequency data in the VLA archive[1] showed that the radio spectrum of the hotspots cuts off very steeply at observing frequencies of tens of GHz (Table 1, Fig. 2). Because it is photons at around these frequencies that are scattered up to X-ray energies, 3C 196 became less attractive as a *Chandra* target. But the cutoff in the synchrotron spectrum does rule out the possibility of an optical synchrotron hotspot. For this reason it is interesting to look for optical inverse-Compton emission in this object.

[1] The National Radio Astronomy Observatory Very Large Array (VLA) is operated by Associated Universities Inc., under co-operative agreement with the National Science Foundation.

Table 1. Radio flux densities for the hotspots of 3C 196

Frequency (GHz)	North (Jy)	South (Jy)	Reference
0.329	6.9	–	1
0.408	7.1 ± 0.4	15.2 ± 0.6	2
1.67	3.420 ± 0.2	5.58 ± 0.3	2
5.0	1.6 ± 0.2	2.5 ± 0.2	2
15.0	0.472 ± 0.02	0.47 ± 0.07	3
22.5	0.123 ± 0.05	–	3

Data tabulated are for the compact component of the hotspot, which in most cases was unresolved. References are: (1) Linfield & Simon (1984) (2) LM (3) This paper, from VLA archive. The N hotspot is partially resolved at 22 GHz, so the flux quoted may be an underestimate.

3C 196 has already been well studied in the optical (e.g. Boissé & Boulade 1990; Cohen et al. 1996), because the quasar lies close to a $z = 0.437$ barred spiral galaxy which gives rise to absorption in HI (Brown & Mitchell 1983; Brown et al. 1988; Briggs, de Bruyn & Vermeulen 2001) and optical lines (Foltz, Chaffee & Wolfe 1988). Because the hotspots lie only ~ 2 arcsec from the quasar nucleus, high resolution is needed to separate any possible optical hotspot emission from the nucleus. The deepest *Hubble Space Telescope* (*HST*) image is presented by Ridgway & Stockton (1997; hereafter RS), and consists of 8 dithered observations of 900 s duration each on the WFC3 chip in the F622W filter. After combining the images and subtracting the PSF, they find some extended emission probably related to the quasar, as well as imaging the foreground spiral galaxy, but do not comment on any possible hotspot emission.

I have obtained the data of RS from the *HST* archive and combined the individual observations, using the IRAF task CRREJ to remove cosmic rays in the pairs of observations with the same pointings followed by the AIPS tasks HGEOM and COMB to stack the four dither directions. In Fig. 1 I show a greyscale of the resulting image. There is a weak but clear source coincident with the northern hotspot, a component which can also be seen on the image of RS. One of the spiral arms of the foreground galaxy crosses the position of the southern hotspot, rendering any discussion of that component impossible.

The flux density of the component coincident with the northern hotspot can be determined by small-aperture photometry. After subtraction of the well-determined sky background and of a locally determined (and more uncertain) correction for the background local to the source, I find the source to contain 133 ± 27 counts in an extraction region with a radius of 3 pixels. Correcting for the effects of the PSF (Holtzman et al. 1995) and for a small amount of Galactic reddening [$E(B-V) = 0.058$, according to the data of Schlegel, Finkbeiner & Davis (1998)] this

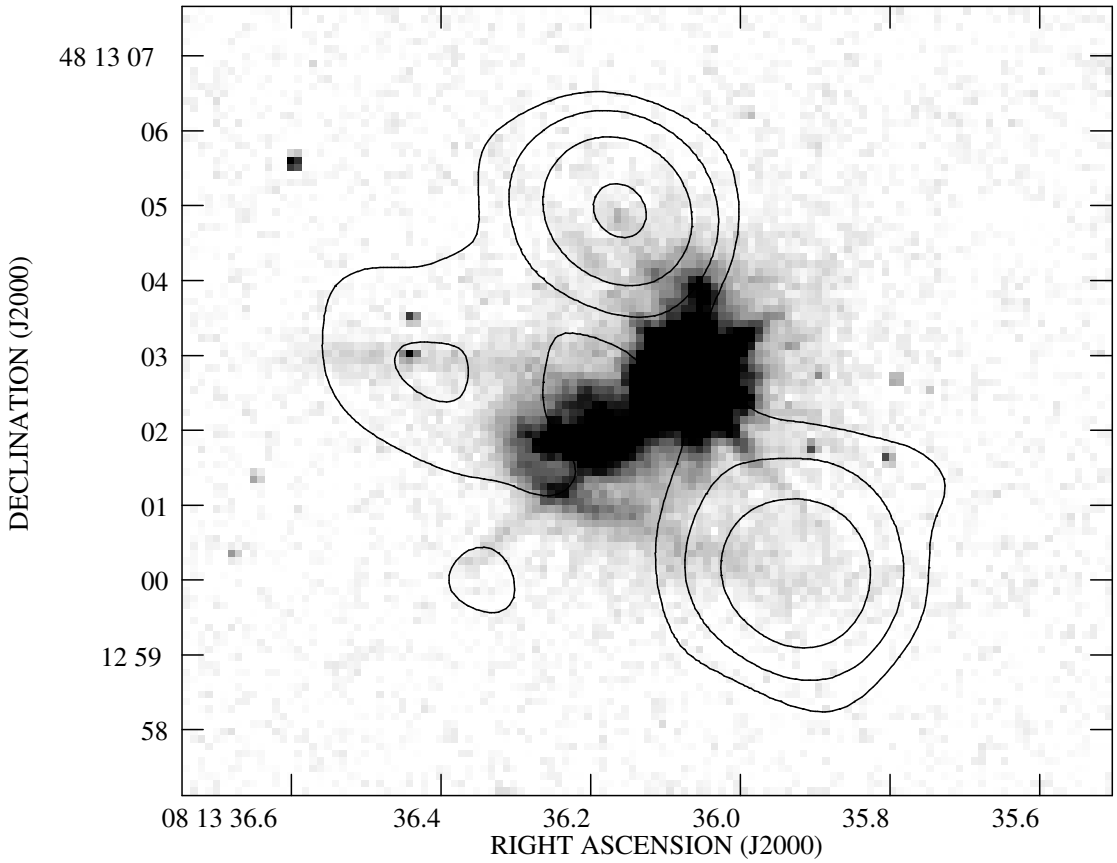

Fig. 1. The WFPC2 (WFC3) image of 3C 196. The linear greyscale range is from 144 to 250 counts per pixel. The PSF has not been subtracted, and its diagonal diffraction spikes can be seen. Below the quasar to the SE is the foreground spiral galaxy. The apparent 'box' to the W of the quasar is the result of a bad pixel on the CCD, and illustrates the dithering strategy used by RS. Radio contours are at $5 \times (1, 4, 16, 64)$ mJy beam^{-1}, taken from a 15-GHz VLA map with a resolution of 1.34×1.09 arcsec. The *HST* positions have been corrected to align the quasar with the radio core.

translates, using factors provided by the IRAF SYNPHOT package, to a flux density of 82 ± 17 nJy at an observing frequency of 4.85×10^{14} Hz.

It is worth briefly considering whether additional reddening might be introduced by the foreground spiral galaxy. The northern hotspot is the component of 3C 196 furthest from the spiral; the separation of 3.1 arcsec corresponds to a distance of 23 kpc at the redshift of the spiral. Observations of optical line absorption against the quasar nucleus show that absorbing material from the spiral certainly has an effect at ~ 10 kpc. On the other hand, we know from the VLBI work of Brown et al. (1988) that the HI column density to the hotspot is $\lesssim 3 \times 10^{20}$ cm^{-2}, which would imply $E(B-V)$ in the frame of the galaxy of $\lesssim 0.06$; this could give up to 0.14 mag of reddening at our observing wavelength, but this would only increase the inferred flux density by 14 per cent, to 93 nJy. The effect is therefore not significant. The detailed models of Briggs et al. (2001) place the northern hotspot outside the absorbed region.

3. Inverse-Compton?

In order to calculate the inverse-Compton flux density expected at this frequency we must assume a size and geometry for the hotspot. To carry out the calculation I use the code of Hardcastle, Birkinshaw & Worrall (1998) which assumes that the hotspot is a homogeneous sphere. The radius of the sphere is set to 0.3 arcsec, based on the MERLIN image of Lonsdale (1984). The synchrotron spectrum is then fit with a simple model consisting of a low-frequency power law with spectral index 0.5 and a high-energy cutoff; this constrains the upper energy of the electrons, and gives an adequate fit to the radio data (Fig. 2). The unknown parameters are then the low-energy cutoff of the electron spectrum, and the magnetic field strength in the hotspot.

The value of the low-energy cutoff has a strong effect on the predicted optical SSC emissivity, because it is the low-energy electrons that scatter radio photons into the optical band. For a given energy density in photons, high cutoffs reduce the optical emissivity, while low cutoffs increase it. A smaller but still significant effect is that a lower cutoff implies a greater energy density in electrons, giving

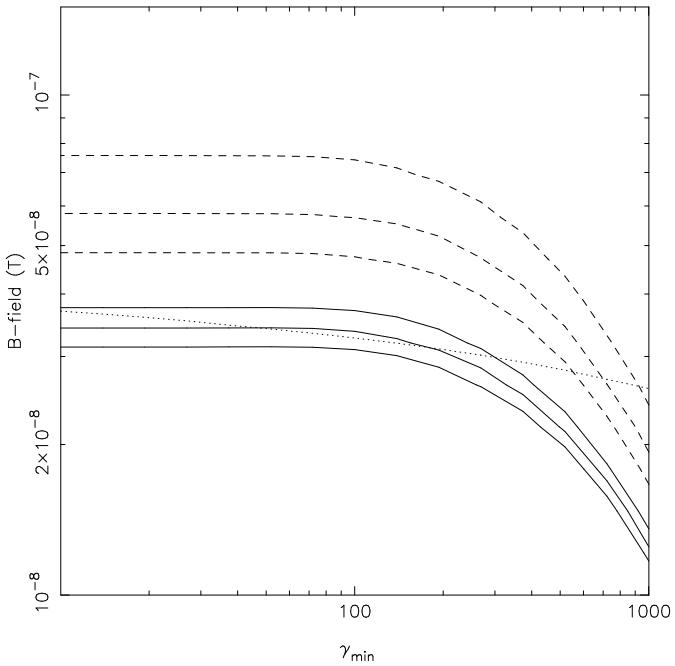

Fig. 3. The difference between predicted and observed values of the optical flux as a function of $\gamma_{\rm min}$ and B. The contours show a difference between prediction and observation of 1, 2 and 3 σ; the solid contours show the model *overpredicting* the observed optical flux, while the dashed contours show where the model *underpredicts* the observations. The dotted line shows the equipartition field strength as a function of $\gamma_{\rm min}$. The values plotted here are for the default cosmology. Other standard choices of cosmological parameters (e.g. $H_0 = 50$ km s^{-1} Mpc^{-1}, $\Omega_{\rm m} = 0.0$, $\Omega_\Lambda = 0.0$) give very similar results.

rise to an increased equiapartition magnetic field strength. The fact that the source is detected at 408 MHz and below constrains the low-energy cutoff; $\gamma_{\rm min} \lesssim 800(B_{\rm eq}/B)^{\frac{1}{2}}$, where $B_{\rm eq}$ is the equipartition magnetic field strength assuming no protons and filling factor unity. The best fits to the entire radio spectrum are given by $\gamma_{\rm min} \approx 600$, which is comparable to the low-energy cutoffs inferred in Cygnus A and 3C 123 (Table 2).

To see what regions of B and $\gamma_{\rm min}$ are consistent with the observed optical emission, I allowed them both to vary over a wide range and determined the difference between the predicted and observed optical flux density. The results are plotted in Fig. 3.

It will be seen that even if we treat the optical emission from the hotspot as unrelated to the inverse-Compton process, and use it to give an upper limit, this calculation constrains the magnetic field strength in the hotspot. The region in the bottom left of Fig. 3, below the solid contours, is excluded at better than the 3σ level by the data, since parameters in this region would produce more optical emission than is observed. This implies, for plausible $\gamma_{\rm min}$, that the magnetic field strength in the hotspot is close to or greater than the equipartition value. If we believe that inverse-Compton emission has actually been detected in this object, then the magnetic field strength implied is very close to the equipartition value if $\gamma_{\rm min} \sim 400$ – 600,

Table 2. Inverse-Compton parameters obtained for 3C 196 and other sources.

Source	$\gamma_{\rm min}$	u_ν ($\times 10^{-11}$ J m^{-3})	$B_{\rm eq}$ (nT)	$B_{\rm SSC}$ (nT)	Ref.
3C 405 A	420	1.0	31	27	1
3C 295 N	800	8.2	63	30	2
3C 123	1000	0.57	17	12	3
3C 196	600	1.3	28	24	4

I tabulate information for hotspot A of Cygnus A and the N hotspot of 3C 295. $\gamma_{\rm min}$ is the value assumed in the calculation; see the text for a discussion of the values applicable to 3C 196. u_ν is the mean energy density in synchrotron photons; Beq is the equipartition magnetic field strength, using assumptions given in the text; $B_{\rm SSC}$ is the field required if the X-ray or optical emission observed is all to be modelled as SSC. References are: (1) Harris et al. (1994); (2) Harris et al. (2000); (3) Hardcastle et al. (2001); (4) this paper. For consistency, all calculations have been carried out using the Hardcastle et al. (1998) code and the cosmological parameters of this paper, so the results quoted here differ slightly from published values.

a plausible fit to the data. If the low-energy cutoff in the electron spectrum is much lower than this, then to avoid producing an optical SSC hotspot brighter than that observed we require magnetic field strengths greater than the equipartition value, although the difference is never very large, and approaches 1σ for $\gamma_{\rm min} \approx 10$; but the radio data are less well fitted by models with low $\gamma_{\rm min}$. Table 2 compares the derived field strengths for 3C 196, on the assumption of $\gamma_{\rm min} = 600$, with those obtained for other sources. The results are broadly similar.

As Brunetti, Setti & Comastri (1997) have pointed out, photons from the active nucleus can also be inverse-Compton scattered to higher energies by electrons in the radio components. The N hotspot in 3C 196 is a projected distance of only 20 kpc from the nucleus, and so the energy density of nuclear photons in the hotspot may be significant. However, the restricted range of electron energies inferred in the hotspot ($500 \lesssim \gamma \lesssim 6000$) mean that only photons in the radio band can be scattered into the optical. The radio nucleus of 3C 196, as we observe it, is unusually weak for a quasar — only 7 mJy at 5 GHz (Reid et al. 1995). Taking into account the effects of beaming in the manner discussed by Hardcastle et al. (2001) I find that, if the quasar is at an angle of less than 45 degrees to the line of sight, extremely high nuclear bulk Lorentz factors ($\gtrsim 25$) are required to make the number spectral density of nuclear radio photons equal to that seen in the hotspot. A model of this sort seems unlikely to be viable for this particular source.

4. Conclusions

A weak optical component coincident with the northern radio hotspot is detected in 3C 196. The radio spectrum makes this component very unlikely to be due to synchrotron emission. If it is used as an upper limit on any optical SSC emission, it requires the magnetic field strength

in the hotspot to be greater than or equal to the equipartition value. If it is taken to be a *detection* of SSC emission, its flux level is in good agreement with a model similar to the one found to work in X-ray detected hotspots; the low-energy cutoff is around $\gamma = 500$ and the magnetic field strength is close to the equipartition value.

This work illustrates the possibility of finding optical inverse-Compton hotspots in deep observations of radio sources. At the time of writing I am not aware of any other sources with bright compact hotspots of which suitable optical observations exist; observers are encouraged to be alert to the possibility of finding such components in their data.

Acknowledgements. I thank Dan Harris for a helpful referee's report on the first version of this paper.

References

Boissé P., Boulade O., 1990, A&A, 236, 291
Briggs F.H., de Bruyn A.G., Vermeulen R.C., 2001, A&A in press astro-ph/0104457
Brown R.L., 1990, in Zensus J.A., Pearson T.J., eds, Parsec-scale Radio Jets, Cambridge University Press, Cambridge, p. 199
Brown R.L., Mitchell K.J., 1983, ApJ, 264, 87
Brown R.L., Broderick J.J., Johnston K.J., Benson J.M., Mitchell K.J., Waltman E.B., 1988, ApJ, 329, 138
Brunetti G., Setti G., Comastri A., 1997, A&A, 325, 898
Carilli C.L., Perley R.A., Dreher J.W., Leahy J.P., 1991, ApJ, 383, 554
Cohen R.D., Beaver E.A., Diplas A., Junkkarinen V.T., Barlow T.A., Lyons R.W., 1996, ApJ, 456, 132
Foltz C.B., Chaffee F.H., Wolfe A.M., 1988, ApJ, 335, 35
Hardcastle M.J., Birkinshaw M., Worrall D.M., 1998, MNRAS, 294, 615
Hardcastle M.J., Birkinshaw M., Worrall D.M., 2001, MNRAS, 323, L17
Harris D.E., Carilli C.L., Perley R.A., 1994, Nat, 367, 713
Harris D.E., et al., 2000, ApJ, 530, L81
Holtzman J., et al., 1995, PASP, 107, 156
Laing R.A., 1982, in Heeschen, D.S., Wade C.M., eds, Extragalactic Radio Sources, IAU Symposium 97, Reidel, Dordrecht, p. 161
Linfield R., Simon R.S., 1984, AJ, 89, 1799
Lonsdale C.J., 1984, MNRAS, 208, 545
Lonsdale C.J., Morison I., 1983, MNRAS, 203, 833 [LM]
Ridgway S.E., Stockton A., 1997, AJ, 114, 511
Reid A., Shone D.L., Akujor C.E., Browne I.W.A., Murphy D.W., Pedelty J., Rudnick L., Walsh D., 1995, A&AS, 110, 213
Schlegel D.J., Finkbeiner D.P., Davis M., 1998, ApJ, 500, 525
Wilson A.S., Young A.J., Shopbell P.L., 2000, ApJ, 544, L27